Chapter 14

Powder Eutectic Materials of Fe-Mn-C-B System for Coatings of Increased Abrasive Wear

Mykhaylo Pashechko, Klaudiusz Lenik,
Joanna Szulżyk-Cieplak and Aneta Duda

Additional information is available at the end of the chapter

http://dx.doi.org/10.5772/66873

Abstract

In this chapter, selected problems of manufacturing coatings with high wear resistance obtained based on eutectic materials of the quaternary Fe-Mn-C-B system are discussed. With regard to the structural state and physico-mechanical properties of eutectic powder alloys and coatings correspond to the composite dispersion-strengthened materials. The formation of a hardened layer with the structure of eutectic on the metal surface is the creation of a new material with certain mechanical properties. The analysis of different material properties and of alloy addition enabled to work out new eutectic powder alloys based on iron of the Fe-Mn-C-B system. In particular, it enabled to determine eutectic ranges and element contents.

Keywords: powder materials, eutectic, coating, wear, quasi-ternary

1. Introduction

One of the basic possibilities for obtaining surface layers with present properties is to apply coatings of powder based on eutectic alloys of, among other systems, the quaternary Fe-Mn-C-B system to specific material. Such materials offer the possibility of selecting multi-component eutectic alloys by alloying with elements such as silicon, nickel, chromium. These components are most frequently used to obtain products with required wear resistance properties of their surfaces. It means that the research on selection of such materials relates to searching for answers concerning the possibility of producing eutectic alloys as a family of multiphase dispersion-strengthened composite alloys with a structural gradient.

2. Materials and methods

The issue discussed in this chapter relates to new materials, particularly resistant to the abrasive wear, and it has been the subject of permanent research for many years. This subject matter is of current interest due to the development and requirements for properties of various friction pairs used under increasingly new conditions. Such steel elements of some machines represent a group of items for which the research is conducted with regard, but not limited, to production of new composites with specified properties of their surface layers. The main issue for their development is the analysis of phase equilibrium systems. This also applies to the manufacture of new powder materials as eutectic alloys.

The equilibrium systems can be used as a basis for determination of phase composition, existence area and possible phase transitions in the production of eutectic alloys. The analysis of physico-chemical properties of alloying elements, considering possible phase transitions in the system, allows the possibilities of introducing elements into a specific alloy to be evaluated and the nature of their impact to be determined.

The production of solid solutions, chemical compounds, mixture of specified elements with proper predetermined structure and alloy content makes it possible to predict the properties of produced alloys based on properties of input components. In other words, there is a specific relationship between the equilibrium system and the properties of alloys. In practice, a lot of useful alloyed materials consist of more than two components, although the literature has mainly described and studied two-component systems and not many three-component ones, and there are almost no studies on systems consisting of a higher number of components [1–3]. Taking into consideration the positive impact of borides and carbides (in particular, iron and manganese ones) on physico-mechanical properties, operating characteristics of materials and surface layers as well as specific features of producing eutectic layers, the equilibrium systems with eutectic transition using specified elements (components) were analysed. The analysis shows that eutectic systems are obtained in Fe-C, Fe-B, Fe-Mn-C, Fe-Cr-C and Fe-Ni-C systems (**Table 1**) [4, 5].

For production of materials with specified properties of resistance to the abrasive wear, Fe_3C carbides as well as Fe_2B, FeB and Cr_2B borides were selected. The selection of carbides and borides as dispersion (strengthening) phases within the structure of alloy is dictated by their high hardness, wear resistance, corrosion resistance and thermal stability. Furthermore, the addition of manganese allows the ductility of Fe_3C iron carbide and produced eutectic alloy to be increased. Mn forms a solid solution with iron, extends the temperature-concentration area of the existence of Fe_3C-Mn_3C carbides and, at the same time, increases the dispersibility of their distribution [6].

In all equilibrium systems, the formation of eutectic areas is caused by the effects of elements such as Fe, Mn, C, B, Si, Ni and Cr. The discussed research is focused on increasing the yield point of surface layers while ensuring their high hardness. This can be achieved owing to formation of various eutectic layers by introducing (alloying) elements to increase the hardness and ductility. In view of the foregoing and by analysing the properties of phase components, most efficient turns out to be the Fe-B-C system followed by the Fe-Mn-C one [7]. Therefore, it is appropriate to produce powder materials and eutectic layers of the Fe-Mn-C-B system.

http://dx.doi.org/10.5772/66873

System	Alloying elements	Content of elements in eutectic alloy wt%	Phase composition of alloy	Melting point, K	
				Eutectic mixture	Alloying element
Fe-B-C	Fe	95.6	α-Fe + Fe_2B + Fe_3C	1373	1811
	B	2.9			2350
	C	1.5			4413
Fe-Mn-C	Fe	97.4–86.6	α-Fe+$(Fe, Mn)_3C$	1473	1811
	Mn	2.2–13			1518
	C	0.4			4413
Fe-Ni-B	Fe	70.2	γ-Fe + $(Fe, Ni)_2B$ + $(Fe, Ni)_3B$	–	1811
	Ni	25.0			1728
	B	4.8			2350
Fe-Cr-C	Fe	88.4	γ-Fe + F_3C + Cr_7C_3		1811
	Cr	8			2122
	C	3.6			4413
Fe-Ni-C	Fe	48	γ-$(Fe, Ni)_2B$ + Fe_3C		1811
	Ni	50			1728
	C	2			4413

Table 1. Characteristics of eutectic alloys formed based on iron and selected elements.

In the Fe-Mn-C system, there is a very durable $(Fe, Mn)_7(B, C)_3$ phase with rhombic structure. Ternary intersection of the Fe-Mn-C system [3] shows that the eutectic existence area is restricted by the carbon content only and, what is more, over a wide range of concentrations (0.2–0.8 wt%), while manganese content is not limited according to iron because of their unlimited solubility in a solid form.

In general, it can be concluded that types of elements and their specific contents in ternary systems are known. The Fe-B-C eutectic alloys contain, respectively, in wt%, 1.5% C and 2.9% B, and the Fe-Mn-C alloys contain 0.4% C and 2.2–13% Mn. As a result, the subject of development of the Fe-Mn-C-B system to identify the possibilities of producing a eutectic mixture, determine the area of its existence as well as its phase composition and content of elements is still of current interest.

Based on the X-ray structural and microstructural examinations and thermal analysis of the Fe-Mn-C-B alloys, the content of elements in the eutectic areas of Fe-Mn-C and Fe-B-C systems was determined (**Table 2**) [7].

Taking into consideration the specificity and technological details of producing eutectic alloys and surface layers as well as the obtained properties, in particular reduction in a tendency to cracking, it is advisable to adopt the same carbon and boron contents as in the Fe-Mn-C eutectic mixture. The elements of the Fe-Mn-C system offer the possibility of alloying with

components such as Ni, Cr, Ni-Cr and others. This allows manufacturing powder materials with diverse properties, i.e. provides the possibility of influencing the properties of surface layers produced.

Element	Fe-Mn-C	Fe-B-C
Fe	73.3–92.5	85.1–92.5
Mn	3.1–23.8	1.6–7.6
C	0.6–6.4	2.6–7.0
B	0.6–2.5	0.2–3.5

Table 2. Contents (wt%) of elements in eutectic areas of Fe-Mn-C and Fe-B-C systems.

Therefore, it is justified to choose iron, manganese, carbon and boron as the basic elements for manufacturing the base eutectic powder material.

Iron— the main material, included in metallic products—forms solid solutions, chemical compounds and is a carbide former. Carbon and boron in combination with iron form eutectic systems as well as iron carbides and borides with high hardness and strength. In addition, the above-mentioned elements are characterised by high diffusive permeability in the process of saturation of iron-based alloys. In combination with iron, they form chemical compounds and interstitial solid solutions. For the eutectic alloys being developed, the elements were selected based on their known interactions in iron-based alloys [1–3, 8].

Manganese is characterised by high similarity to iron, and it can exchange with it very easily in carbides, at the same time increasing their ductility and dispersion while maintaining rather high strength and thermocyclic stability. Thus, manganese is a very good carbide former. Manganese carbides Mn_3C and iron carbides Fe_3C dissolve in each other, with virtually no limitations. Manganese in combination with iron forms a solid solution. Manganese atoms may substitute iron atoms in Fe_3C carbides. When manganese content is increased in steel, its quantity also increases in carbides, while maintaining a constant ratio of 4:1. In low-carbon steels, carbon content in carbides is much higher than that in high-carbon ones. This difference can be explained by the absolute amount of carbide particles in steel and the related difference in depletion of α-solid solution of iron with manganese. The depletion grows with the increase in amount of carbide particles, and thus carbon content in steel. This is because the basic factor that determines manganese content in carbide is not its amount in steel, but the ratio of equivalent amount of manganese in solid solution to the amount of carbon particles being formed. The weight content of manganese in carbides for steels containing approx. 1% C varies from 0 to 2%, while increasing manganese content in steel from 0 to 50%, respectively (ratio of 4:1). The equivalent content of manganese carbide can only be achieved as a result of rather long steel holding of steel at high temperatures (approx. 1000 K). Manganese extends the area of the existence of γ iron. In particular, manganese increases carbon solubility in γ solid solution at high temperatures. With increasing manganese content, the carbide transition point shifts towards the area of low-carbon contents. Manganese favours shifting of the γ-α transition towards low temperatures. At the same time, the rate of ongoing diffusion processes

http://dx.doi.org/10.5772/66873

decreases, which reduces the rate of the transformation of austenite to martensite. It can be noticed that increasing manganese content in steel makes the degree of pearlite dispersion increase. However, manganese shows no visible impact on the steel hardness after quenching, tempering stability, cutability and heat resistance, which results from the absence of manganese carbides in steels.

During the formation of boride phases in surface layers, e.g. Fe_2B phase, boron atoms are transformed into Sp^2 electron configurations, which try to turn into even more energetic equivalent Sp^3 configurations. Therefore, iron tends to give some of its electrons to boron atoms and turn into a more equivalent state with formation of stable d^5 configurations. In the state of isolated atoms, boron and iron show the following configuration of valence electrons: $2s^22p^1$ and $3d^64s^2$ [2]. As a result of the electron exchange and formation of energetically stable Sp^3 and d^5 configurations, strong covalent compounds are formed between iron and boron atoms. It means that the boride phase, which shows high degree of localisation of the atomic valence electrons, is characterised by relatively high hardness, wear resistance and corrosion resistance.

With the increase in principal quantum number of valence Sp electrons, the stability of Sp^3 boron electron configuration is reduced, and thus the reliability of their occurrence is reduced too. The iron compounds containing silicon that form in the surface layer show considerably lower microhardness than iron borides.

Borides are characterised by significant resistance to abrasive wear compared to high-melting carbides and oxides. Wear resistance of boride-based surface layers decreases due to their high brittleness. In surface layers containing a slight amount of borides, wear resistance is also reduced due to the existence of a large amount of core (matrix) material. It follows that the eutectic layers containing metal borides may be characterised by high ductility, hardness, durability and significant resistance to abrasive wear.

Boron is added to practically all heat-resistant nickel-based alloys for casting in the amount of 0.01–0.10% to strengthen the grain boundaries. It shows poor solubility in nickel. First of all, it dissolves according to the grain boundaries, at contents exceeding 0.015%. Along the grain boundaries, it is precipitated as borides, thus forming the eutectic mixture. Its reinforcing effect is realised mainly by inhibiting diffusion processes at the grain boundaries. This reduces the strength of the alloys, which is connected with formation of TiB_2, CrB_2 (Mo, W, Cr)$_3B_2$ borides that practically contain no basic element—nickel.

The heat treatment being conducted has virtually no effect on the hardness of carbides and borides.

By changing the amounts of iron and ferromanganese, the eutectic degree of surface layers can be controlled. Adding B, Ni, Cr, Fe, Si, Cu, FeSi, FeB and other compounds to the base mixture makes it possible to develop a group of mixtures for forming surface layers with various properties. It allows selecting the range of mixture components to enhance the ability to saturate the surface layer while maintaining a relatively high hardness, wear resistance and ductility of produced layers. Taking into account the discussed effects, the base system of elements, i.e. Fe-Mn-C-B, as well as the area of the existence of eutectic and details of its formation were selected and defined. Based on the above-mentioned base system, the possibility of forming

materials with defined phase composition as well as properly controlled physical, chemical and mechanical properties and operating characteristics was adopted.

The developed eutectic materials were made as a powder based on iron of the Fe-Mn-C-B system for build-up welding or spraying with partial melting of the surface layer. In these processes, this may cause their insufficient deoxidation, which, in turn, may adversely affect the formation of strengthened surface layer. To prevent the potential occurrence of the above-mentioned negative effects, boron and silicon were adopted as the elements to counteract oxidation. The enhancement of diffusion properties of eutectic alloys, in particular carbon, can be achieved by addition of silicon. Silicon forms limited solid solutions with iron and manganese. In recent years, much emphasis is placed on the development of self-deoxidising iron-based alloys containing boron and silicon. These materials replace expensive toxic deoxidisers, improve working conditions, simplify technologies and increase the efficiency of surface treatment by various methods. Thus, boron and silicon can be considered together with manganese as the perspective elements for production of low-cost surface layers compared to alloys in the form of nickel-based powder [5, 6].

Silicon favours the formation of boron from B_2O_3 and production of increased amount of Fe_2B iron boride within the structure of eutectic layers. The applied silicon content in eutectic layers [9] varies between 1.2 and 9.75 wt%. Due to the impact of silicon as deoxidiser and enriching the solution with iron atoms during the partial melting of treated material, its local content in the eutectic layer varied between 0.1 and 5%. The applied silicon concentration along the layer's depth varies between 1 and 2%. At FeSi content of 13% in the mixture (0.1–5 wt% per layer), the surface layer of Fe-Mn-C-B system with increased Fe_2B content is formed. At a lower silicon content in the mixture, layers with sub-eutectic structure are produced. The use of silicon in the base system is due to the fact that it is a good deoxidiser, and together with manganese and boron it enhances self-oxidation of powder materials. Self-oxidation is necessary, particularly, while forming the surface layers by build-up welding, spraying or spraying with partial melting of the surface layer, when there is no possibility of introducing additional self-oxidising elements, like, for example, the use of B_2O_3 in build-up welding with high-frequency currents. Therefore, it is necessary to use silicon for alloying the base powder Fe-Mn-C-B system.

Iron in combination with silicon forms solid solutions (maximum silicon content is approx. 1.5%), which are characterised by good resistance to various acids and high temperatures. Steels usually contain very low amounts of silicon (0.0–1.3%). The impact of silicon on properties is slight if ignoring its effect as a deoxidiser, which is similar to that of manganese. At contents of 0.5–0.6% and above, silicon is considered as an alloying element, which increases hardness and ultimate strength of alloys at high temperatures and corrosion resistance at low temperatures and reduces ductility. When reducing silicon content within the areas of γ-solutions in alloys containing more than 3 wt% Si, there are no phase transitions up to the melting point.

In selection of elements, it is taken into consideration that silicon is the second most important component after carbon in cast irons. By reducing silicon content, the graphitisation coefficient of cast iron can be controlled. Already at Si content of 4% and more, practically all cast irons used in thin-walled casts are replaced with cast irons with grey cast iron structure. The castable cast

http://dx.doi.org/10.5772/66873

irons usually contain 1.25–4.2% Si, while the workable ones contain 0.2–2% Si, which is taken into consideration when selecting the amounts of silicon and boron in eutectic alloys.

Silicon quickly reduces the amount of carbon in eutectic mixture. At Si content of 16%, hyper-eutectic are even alloys containing 0.6–1.0% C. Alloys containing 14–16% Si are characterised by high-corrosion resistance, and hence they are commonly used in the chemical industry.

Silicon is an element, which significantly reduces the diffusion coefficient of carbon in the α- and γ-crystal lattice. In steel, carbides contain a small amount of silicon as its atoms are quickly moved from carbides to solid solution. Silicon is not a typical carbide former. In alloys with high silicon content (20–23% Si), SiC carbide is formed. Therefore, the limit of alloying eutectic alloys with silicon is assumed to be approx. 3–4% because the ductility of eutectic alloys decreases at its greater contents.

For examinations of the Fe-Mn-C-B phase equilibrium system, the preparation of samples from carbonyl iron (99.99%), manganese (99.5%), amorphous boron (99.3%) and synthetic graphite (99.94%) powders by alloying in an electric furnace in a purified argon atmosphere was adopted. The annealing of samples was carried out in vacuum quartz containers at 1273 K for 350 h. To determine samples with a eutectic structure, thermal and metallographic tests (Neophot-2 MIM-8, DAT, AT) were carried out and the concentration of elements ('Kamebax,' Superprobe-733) in alloys in the as-annealed (1273 K, 350 h) and standardised condition was analysed. Based on obtained data, a quasi-ternary Fe-Mn-C-B-Si system was developed (**Figure 1**). The component contents in individual intersections were changed every 10 molar parts. The area of iron concentration was 0.67–0.79 at% [6, 8].

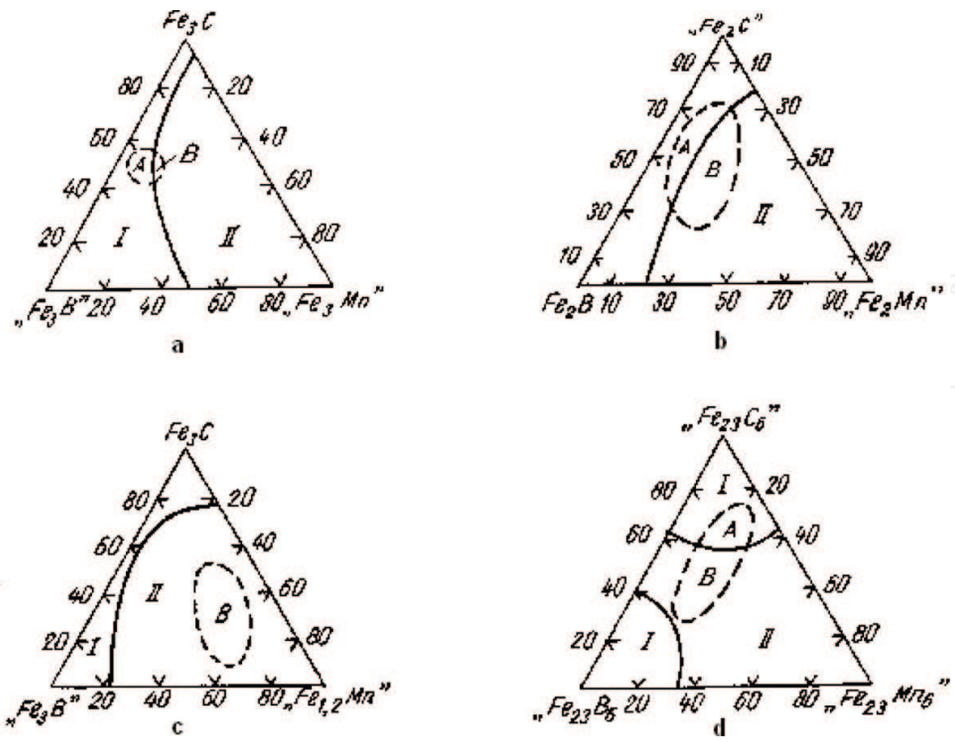

Figure 1. Phase areas (I, II, A, B) in quasi-ternary intersections: (**a**) Fe_3C-Fe_3B-'Fe_3Mn', (**b**) 'Fe_2C'-Fe_2B-'Fe_2Mn', (**c**) Fe_3C-Fe_3B-'$Fe_{1.2}Mn$', (**d**) '$Fe_{23}C_{6'}$-'$Fe_{23}B_{6'}$-'$Fe_{23}Mn_{6'}$.

For evaluation of the structure and phase composition of elements, the X-ray analysis of phase composition of the alloys produced and the micro-X-ray structural analysis of the content of elements was carried out.

The obtained effects of structural analyses of the alloys, in particular their phase composition and content of elements, are presented as a description of phase areas, I and II, and areas of the existence of Fe-Mn-C and Fe-B-C eutectics, A and B, in four quasi-ternary intersections (**Figure 1a–d**) [9].

3. Result and discussion

3.1. Examination and analysis of Fe_3C–Fe_3B–'Fe_3Mn' quasi-ternary intersection

In order to determine the phase areas and content of elements, the micro-X-ray and micro-structural examinations of the Fe_3C–Fe_3B–'Fe_3Mn' quasi-ternary intersection were carried out. Based on the examinations performed, two phase areas were identified (**Figure 1a**; **Table 3**). Area I consists of $Fe_3(B, C)$, α-(Fe, Mn), γ-(Fe, Mn), and area II consists of α-(Fe, Mn), γ-(Fe, Mn), $(Fe, Mn)_{23}(C, B)_6$, $(Fe, Mn)_2B$.

As a result of micro-X-ray examinations, the following content of elements in hypereutectic alloys was determined (in at%): 67.8–75.0 Fe, 1.2–4.5 Mn, 8.5–14.3 B, 11.0–13.9 C [6, 10].

The quasi-ternary intersection of the equilibrium system was examined for 19 samples, annealed at 1273 K. In the analysed intersection, the $(Fe, Mn)_{23}(C, B)$ and $(Fe, Mn)_3(B, C)$ phases with $Fe_{23}C_6$ and Fe_3C structures, respectively, were established. For example, sample nos. 6 and 10 contain a phase with cementite structure the lattice of which has the following parameters: a = 0.5341, b = 0.6650, c = 4.459 nm. Parameters of the cementite structure phase lattice correspond to those of Fe_3C. Samples 1–4 and 11 contain the Fe_3C phase only with increased lattice parameters, which corresponds to those of $Fe_3(B,C)$ borocarbide. Some of the samples include the $(Fe, Mn)_{23}(B, C)_6$ phase, Fe_2B-$(Fe, Mn)_2B$-based solid solution. The peculiarity of sample nos. 1–8, 10, 11, 15, 17, 18, 19 (**Table 3**) is that they include the α-(Fe, Mn) solid solution. The obtained phase composition of hypereutectic alloy samples is presented in **Table 3**.

As it can be seen in **Table 3**, for phase area I (**Figure 1a**), the hypereutectic alloy is formed in sample no. 3 only, whereas all other samples represent solid solutions.

As it was determined from experimental metallographic and X-ray structural examinations of the alloys, sample no. 3 $Fe_{75}Mn_{3.6}B_{10}C_{12.5}$ is a hypereutectic alloy composed of $Fe_3(B, C)$ + α-(Fe, Mn) eutectic between which $Fe_{0.4}Mn_{3.6}C$ iron-manganese carbides are arranged. The second grade dendrites are arranged in the crystallographic direction [11] (**Figure 2a**). The annealing of $Fe_{75}Mn_{3.6}B_{10}C_{12.5}$ alloy at 1273 K for 350 h results in the formation of pearlitic grooves (**Figure 2b**). In carbon-enriched alloys, the $Fe_{0.4}Mn_{3.6}C$ iron-manganese carbide lamellas of 15–35 μm in length are formed (**Figure 2c**). A strip of the second eutectic phase—pearlite—is formed on the lamella surface and grows along the surface. It has the appearance of a flat den-

http://dx.doi.org/10.5772/66873

drite. The results of the examinations confirm that in the crystallisation process, the leading phase in the phase carbon-solid solution eutectics is always carbide crystals. The structure of other examined samples—α- and γ-(Fe, Mn)-based solid solutions with $Fe_3(C, B)$, $(Fe, Mn)_2B$ borocarbide or $(Fe, Mn)_{23}(C, B)_6$ carbide inclusions. The Fe-B-C eutectic exists in area A, while the Fe-Mn-C eutectic is observed in area B (**Figure 1a**).

Sample number	Component contents; molar part 10			Phase composition	Alloy type	Phase area (Figure 1a)
	Fe_3C	"Fe_3B"	"Fe_3Mn"			
3	5	4	1	$Fe_3(B, C)$ + α-(Fe, Mn) + trace amount of γ-(Fe, Mn)	Hyper-eutectic alloy	I
1	1	8	1	$Fe_3(B, C)$ + trace amount of α-(Fe, Mn)	Solid solution	
2	3	6	1			
6	2	6	2			
4	7	2	1	$Fe_3(B, C)$ + α-(Fe, Mn)	Solid solution	
10	1	6	3			
11	3	4	3			
5	8	1	1	α-(Fe, Mn)+$(Fe, Mn)_2B$+$(Fe, Mn)_{23}(C, B)_6$	Solid solution	II
8	6	2	2			
7	4	4	2	α-(Fe, Mn) + traces of transient phase +$(Fe, Mn)_{23}(C, B)_6$+ γ-(Fe, Mn) + trace amount of α-(Fe, Mn)	Solid solution	
15	2	3	5			
18	2	2	6			
17	4	1	5	$(Fe, Mn)_{23}(C, B)_6$ +γ-(Fe, Mn) + α-(Fe, Mn)	Solid solution	
19	1	2	7			
16	3	2	5	$(Fe, Mn)_{23}(C, B)_6$ + γ-(Fe, Mn)	Solid solution	

Table 3. Phase composition of Fe-Mn-C-B samples with iron content of 0.75 at%.

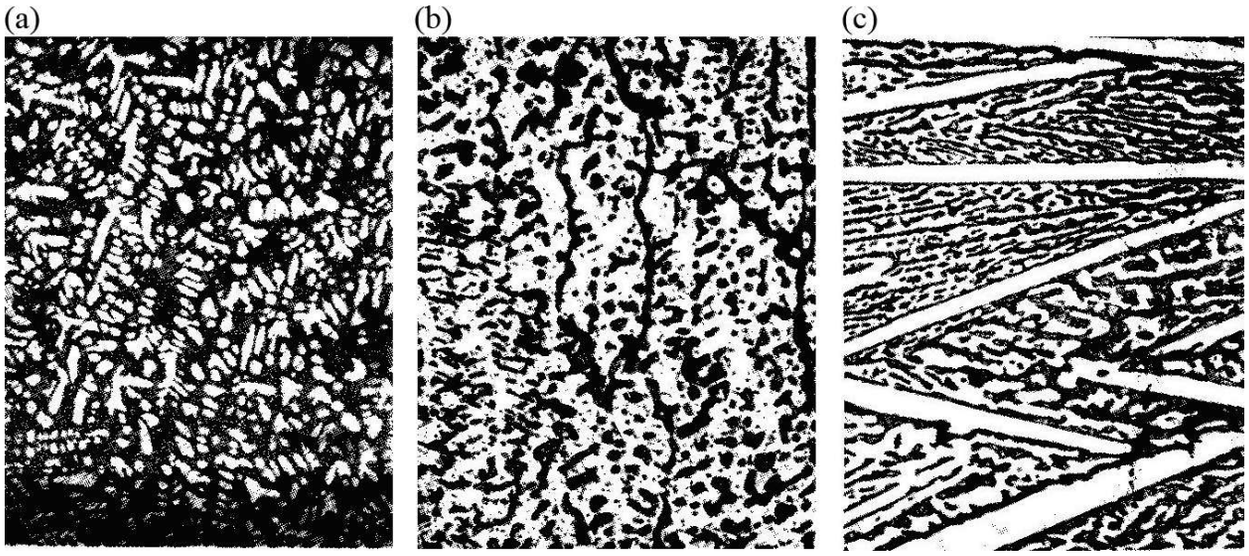

Figure 2. Microstructure (×200) of the examined samples (markings according to **Table 3**), hyper-eutectic alloy (sample no. 3, a, b) and solid solution [sample no. 5 (c)]; (a) after normalising; (b,c) after annealing (at 1273 K, 350 h).

3.2. Examination and analysis of 'Fe$_2$C'–Fe$_2$B–'Fe$_2$Mn' quasi-ternary intersection

To determine the phase areas and the content of elements, the examinations of 'Fe$_2$C'–Fe$_2$B–'Fe$_2$Mn' intersection samples (**Figure 1b**) containing the Fe$_3$(B, C), Fe$_2$B, γ-(Fe, Mn) and (Fe, Mn)$_{23}$(C, B)$_6$ phases were carried out. Phase composition of the samples with iron content of 0.667 at% is presented in **Table 4**.

Based on the micro-X-ray and microstructural examinations performed in the 'Fe$_2$C'–Fe$_2$B–'Fe$_2$Mn'quasi-ternary intersection, two phase areas were identified (**Figure 1b**; **Table 4**). Area I consists of Fe$_3$(C, B) and area II consists mainly of (Fe, Mn)$_{23}$(C, B)$_6$ + γ-(Fe, Mn). Hypereutectic alloys are in area II (**Figure 1b**). The Fe-B-C eutectic exists in area A, while the Fe-Mn-C eutectic is observed in area B (**Figure 1b**). Content of elements in hypereutectic alloys (at%): 66.7 Fe, 3.3–6.7 Mn, 10.0–23.3 C, 6.7–16.6 B. In hypereutectic alloys (sample Nos 3–4), the primary Fe(B, C) crystals and (Fe, Mn)$_{23}$(C, B) iron-manganese carbide dendrites are formed, **Figure 3a** and **b**. No borocarbide inclusions were identified. In boron-enriched alloys, the primary austenite crystals are formed. In γ-(Fe, Mn)-(Fe, Mn)$_{23}$(C, B)$_6$ eutectic alloys, the micro-areas of γ-(Fe, Mn) solid solution and austenite dendrites were revealed. In alloys containing an increased amount of manganese, the primary dendrites (Fe, Mn)$_{23}$(C, B)$_6$ are formed (**Figure 3c**). Content of elements in eutectic alloys (at%): 66.6 Fe, 1.7–11.0 Mn, 7.7–25.0 C, 4.0–8.4 B [4, 9].

3.3. Examination and analysis of Fe$_3$C-Fe$_3$B-'Fe$_{1.2}$Mn' quasi-ternary intersection

In the examined quasi-ternary intersection, most of the Fe$_3$C-Fe$_3$B-"Fe$_{1.2}$Mn" samples (**Figure 1c**) comprise the (Fe, Mn)$_{23}$(C, B)$_6$ phase, which is in equilibrium with the Fe$_3$(B, C) and γ-(Fe, Mn) or γ-(Fe, M) phase. According to the results of phase analysis, the (Fe, Mn)$_{23}$(C, B)$_6$ + γ-(Fe, Mn) + Fe$_3$(C, B) phase area is visible very well [7, 8]. The samples contain no α-Fe-based phase. Phase composition of the samples is presented in **Table 5**. The most complex structure (number of phases) is visible in sample nos. 4, 24.

http://dx.doi.org/10.5772/66873

Sample number	Component contents; molar part 10			Phase composition	Alloy type	Phase area
	'Fe$_2$C'	Fe$_2$B	'Fe$_2$Mn'			
1	1	8	1	Fe$_3$(C, B)	Solid solution	I
2	3	6	1	„	-"-	
3	5	4	1	„	Hyper-eutectic alloy	
4	7	2	2	„	-"-	
5	7	2	2	Fe$_3$(C, B)	Solid solution	II
9	1	1	1	(Fe, Mn)$_{23}$(B, C)$_6$ + Fe$_2$B + Fe$_3$(B, C)	Solid solution	
6	3	5	2	(Fe, Mn)$_{23}$(B, C)$_6$ + Fe$_2$B + Fe$_3$(B, C)	Hyper-eutectic alloy	
7	5	3	2	(Fe, Mn)$_{23}$(B, C)$_6$+γ-(Fe, Mn)	Hyper-eutectic alloy	
10	5	2	3	(Fe, Mn)$_{23}$(C, B)$_6$+γ-(Fe, Mn)	Solid solution	
11	1	5	4	„	„	
12	3	3	4	„	„	
13	5	1	4	„	„	
15	2	2	6	„	„	
14	1	3	6	γ-(Fe, Mn)+(Fe, Mn)$_{23}$(C, B)$_6$	Solid solution	
16	3	1	6	„	„	
17	1	1	6	„	„	
8	7	1	2	γ-(Fe, Mn)	Solid solution	

Table 4. Phase composition of Fe-Mn-C-B samples with iron content of 0.667 at% ('Fe$_2$C'-Fe$_2$B-'Fe$_2$Mn' intersection (**Figure 1b**)).

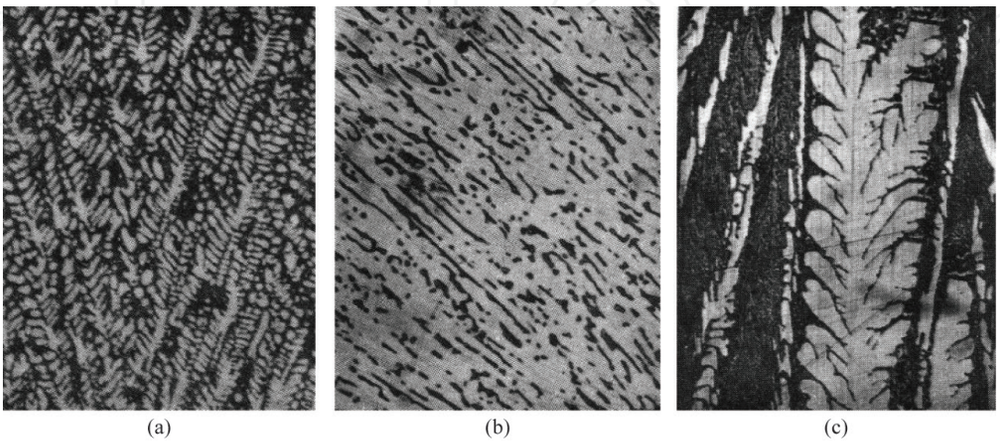

Figure 3. Microstructure (×200) of the examined 'Fe$_2$C'-Fe$_2$B-'Fe$_2$Mn' quasi-ternary intersection alloys (markings according to **Table 4**): sample no. 3 (a, b), sample no. 10 (c); (a, c) after normalisation; (b) after annealing at 1273 K, 350 h.

Sample number	Component contents; molar part 10			Phase composition	Alloy type	Phase area
	Fe_3C	Fe_3B	'$Fe_{1.2}Mn$'			
6	1	7	2	$(Fe, Mn)_{23}(C, B)_6$ + small amount of $Fe_3(B, C)$	Solid solution	I
1	1	8	1	$Fe_3(C, B)$ + γ-(Fe, Mn)	-"-	
2	2	7	1	$Fe_3(B, C)$	-"-	
5	8	1	1	-"-	-"-	
13	2	2	3	$(Fe, Mn)_{23}(B, C)_6$+γ-(Fe, Mn)	Sub-eutectic	II
20	4	1	5	-"-	Solid solution	
21	1	3	6	-"-	-"-	
3	4	5	1	-"-	-"-	
7	3	5	2	-"-	-"-	
12	3	4	3	-"-	-"-	
14	6	1	3	-"-	-"-	
16	3	3	4	-"-	-"-	
17	5	1	4	-"-	-"-	
22	2	2	6	$(Fe, Mn)_{23}(B, C)_6$+ trace amount of γ-(Fe, Mn)	-"-	
26	1	1	8	-"-	-"-	
25	2	1	7	$(Fe, Mn)_{23}(B, C)_6$+ small amount of γ-(Fe, Mn)	-"-	

Table 5. Phase composition of Fe-Mn- C-B samples, Fe_3C + Fe_3B + '$Fe_{1.2}Mn$' intersection (**Figure 1c**).

Based on the micro-X-ray and microstructural examinations performed in the Fe_3C-Fe_2B-'$Fe_{1.2}Mn$' quasi-ternary intersection, two phase areas were identified (**Figure 1c**; **Table 5**). Area I consists of $(Fe, Mn)_{23}(C, B)_{6'}$ $Fe_3(C, B)$ and γ-(Fe, Mn) and area II consists of $(Fe, Mn)_{23}(C, B)_{6'}$ γ-(Fe, Mn) and $Fe_3(B, C)$. Sub-eutectic alloys are in area II (**Figure 1c**). In the intersection determined, there is only the Fe-Mn-C eutectic in area B (**Figure 1c**).

In manganese-enriched sub-eutectic alloys, the primary dendrites γ-(Fe, Mn) are formed and the $(Fe, Mn)_{23}(C, B)_6$+γ-(Fe, Mn) eutectic is arranged between them (**Figure 4a**). The annealing of alloys results in homogenisation and coagulation of γ-(Fe, Mn) crystals (**Figure 4b**). Content of elements in sub-eutectic alloys (at%): 65.3–71.1 Fe, 8.7–21.5 Mn, 2.8–15.4 C, 2.9–10.4 B.

3.4. Examination and analysis of '$Fe_{23}C_{6'}$- '$Fe_{23}B_{6'}$-'$Fe_{23}Mn_{6'}$ quasi-ternary intersection

To determine the phase areas and the content of elements, the examinations of '$Fe_{23}C_{6'}$-'$Fe_{23}B_{6'}$-'$Fe_{23}Mn_{6'}$ intersection (**Figure 1d**) containing the phase with carbide structure $(Fe, Mn)_{23}(C,B)_6$

http://dx.doi.org/10.5772/66873

in Fe-B-C i Fe-Mn-C ternary systems, which restrict the examined intersection, were carried out. The highest number of phases in equilibrium is found in phase area II—(sample no. 7) $(Fe, Mn)_{23}(B, C)_6$ + α-(Fe, Mn) + $Fe_3(B, C)$ and in phase area I—(sample no. 10) $Fe_3(B, C)$ + traces of α-(Fe, Mn) + γ-(Fe, Mn). Samples 4, 5, 7, 10 and 19 (**Table 6**) comprise the ternary phase $Fe_3(B, C)$ [7]. Some of the samples comprise the quaternary phase $(Fe, Mn)_{23}(C, B)_6$. At the intersection of Fe-Mn-C-B system, at Fe content of 0.79 atomic parts, the phase equilibrium of $(Fe, Mn)_{23}(C, B)_6$ + $Fe_3(C, B)$ + γ-(Fe, Mn) + γ-(Fe, Mn) was identified too. In particular, the γ-(Fe, Mn) phase was observed in samples 2, 5, 7, 9, 10 and 11 (**Table 6**).

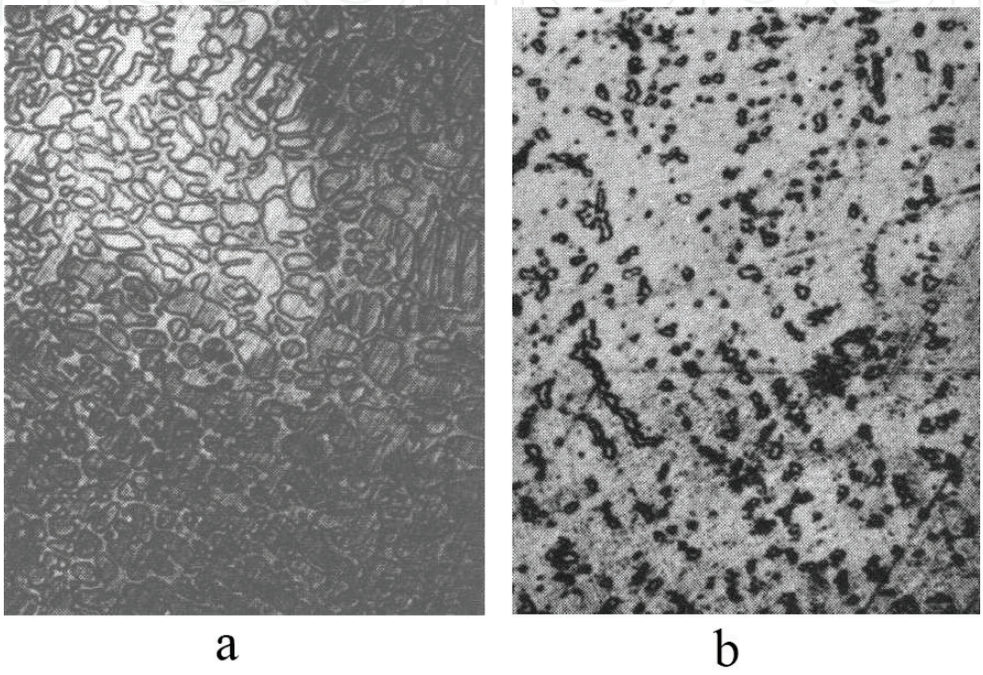

Figure 4. Microstructure (×200) of the examined Fe_3C-Fe_3B-'$Fe_{1.2}Mn$' quasi-ternary intersection alloys (markings according to **Table 5**): (a) sample no. 13, sub-eutectic alloy after normalising; (b) solid solution, sample no. 20, after annealing at 1273 K, 350 h.

Sample number	Component contents molar part 10			Phase composition	Alloy type	Phase area
	'$Fe_{23}C_6$'	'$Fe_{23}B_6$'	'$Fe_{23}Mn_6$'			
7	3	5	2	$(Fe, Mn)_{23}(B, C)_6$+ α-(Fe, Mn)+$Fe_3(B, C)$	Sub-eutectic	II
9	5	3	2	$(Fe, Mn)_{23}(B, C)_6$ + trace amount of α- Fe	-"-	
11	1	6	3	γ-(Fe, Mn)+$Fe_3(B, C)$ + $(Fe, Mn)_{23}(B, C)_6$ + α-(Fe, Mn)	-"-	
3	5	4	1	$(Fe, Mn)_{23}(B, C)_6$	-"-	
12	2	4	3	$(Fe, Mn)_{23}(B, C)_6$ + γ-(Fe, Mn)	Solid solution	
13	5	2	3	-"-	-"-	
32	2	2	6	γ-(Fe, Mn) + $(Fe, Mn)_{23}(B, C)_6$	-"-	
23	3	1	6	-"-		

Sample number	Component contents molar part 10			Phase composition	Alloy type	Phase area
	'$Fe_{23}C_6$'	'$Fe_{23}B_6$'	'$Fe_{23}Mn_6$'			
2	3	4	3	α-Fe + Fe_{23}(B, C)	-"-	I
4	7	2	1	Fe_3(B, C)	-"-	
5	8	1	1	Fe_3(B, C) + trace amount of α- Fe	-"-	
10	7	1	2	Fe_3(B, C) + trace amount of α - (Fe, Mn) +γ-(Fe, Mn)	Sub-eutectic	
19	3	2	5	γ-(Fe, Mn) + α- (Fe, Mn) + Fe_3(B, C)	-"-	

Table 6. Phase composition of Fe-Mn-C-B samples; intersection at iron content of 0.79 at%.

Based on the micro-X-ray and microstructural examinations performed in the 'Fe_{23}C'-Fe_{23}B-'Fe_{23} Mn'quasi-ternary intersection, two phase areas were identified (**Figure 1d**; **Table 6**). Area I consists of Fe_3(C,B), α-(Fe, Mn), γ-(Fe, Mn) and α-Fe and area II consists of $(Fe, Mn)_{23}(C, B)_6$, α-(Fe, Mn), γ-(Fe, Mn) and Fe_3(B, C). Sub-eutectic alloys are in areas I and II (**Figure 1d**). The Fe-B-C eutectic exists in area A, while the Fe-Mn-C eutectic is observed in area B (**Figure 1d**).

Content of elements in sub-eutectic alloys (at%): 79.3 Fe, 2.7–6.2 Mn, 5.4–15.5 C, 1.1–10.8% B. In sub-eutectic alloys, austenite dendrites are formed at elevated carbon contents, while at lower carbon contents, pearlite dendrites are formed (**Figure 5a**). Austenite dendrites are evenly distributed throughout the alloy volume. The annealing of subeutectic alloys results in coagulation of γ-(Fe, Mn) crystals (**Figure 5b**).

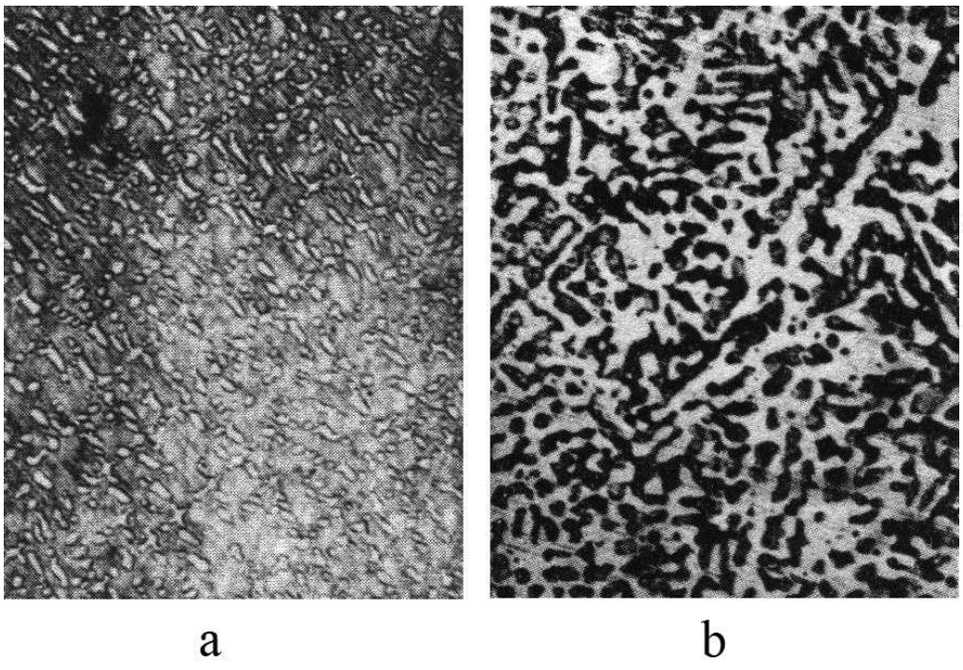

Figure 5. Microstructure (×200) of sub-eutectic alloy, sample no. 7 (markings according to **Table 6**); (a) after normalising; (b) after annealing at 1273 K, 350 h.

http://dx.doi.org/10.5772/66873

By comparing the nature of the effects of components, it can be concluded that the $(Fe, Mn)_{23}(C, B)_6$ phase was found at all intersections. As a pure phase, it exists at Fe content of 0.79 at% (molar parts°10): $5Fe_{23}C_6Fe_{23}Mn_6 4Fe_{23}B_6$-$4Fe_3CFe_{1.2}Mn5Fe_3B$, intersection Fe_3C-Fe_3B-$Fe_{1.2}Mn$.

The areas were identified where quaternary borocarbide is included as the basic phase: (3–4) Fe_3B(4–5)Fe_3Mn(2–3)Fe_3C-$Fe_3B8Fe_3Mn2Fe_3C$ at Fe content of 0.75 atomic parts and (1–5) Fe_2B4Fe_2Mn(1–5)Fe_2C-(2–3)Fe_2B(2–6)Fe_2Mn(2–5)Fe_2C at Fe content of 0.667 atomic parts. A relationship was observed according to which with the reduction in iron content, the area of the existence of $(Fe, Mn)_{23}(C, B)_6$ phase moves towards the area of higher manganese and boron contents and lower carbon content (**Figure1a** and **b**).

Based on theoretical assumptions and experimental verification, the areas of the existence of Fe-Mn-C-B eutectic, as a new family of dispersion-strengthened eutectic alloys with a structural gradient, were identified. The areas of the existence (**Figure 1**; **Table 7**) of hyper- and sub-eutectic alloys were identified too.

Quasi-ternary intersection		**Content of elements***			
		Fe	**Mn**	**C**	**B**
System	Fe-Mn-C-B	73.3 – 92.5 65.3-79.3	1.6–23.8 1.2-21.5	0.6–7.0 2.8-25.0	0.2–3.5 1.1-18.4
Eutectic	Fe-Mn-C	73.3–92.5 65.3-79.3	3.1–23.8 2.7-21.5	0.6–6.4 2.8-23.4	0.6–2.5 2.9-18.4
Eutectic	Fe-B-C	85.1–92.5 66.6-79.3	1.6–7.6 1,2-6,2	2.6–7.0 10,5-25,0	0.2–3.5 1,1-17,7
Intersection	Fe_2C-Fe_2B-"Fe_2Mn"	81.2–89.2 66.6	2.2–13.1 1,7-11,0	2.0–7.0 7,7-25.0	0.9–4.5 4,0-8,4
Eutectic	Fe-Mn-C	81.2–86.3 66.6	6.0–13.1 4.7-11.0	2.0–6.4 7.7-23	0.9–4.6 4.0-18.4
Eutectic	Fe-B-C	85.1–89.2 66.6	2.2–7.6 1.7-6.0	3.0–7.0 11.0-25.0	0.9–4.4 4.0-17.7
Intersection	Fe_3C-Fe_3B-"Fe_3Mn"	87.1–92.5 67.8-75.0	1.6–5.7 1.2-4.5	2.8–3.7 11.0-13.9	1.9–3.5 8.5-14.3
Eutectic	Fe-Mn-C	90.1–91.2 75.0	3.3–4.8 2.8-4.0	2.8–3.5 11.0-13.7	1.9–2.4 8.5-10.0
Eutectic	Fe-B-C	87.1–92.5 67.8-75.0	1.6–5.7 1.2-4.5	2.8–3.7 11.0-13.9	2.0–3.5 8.5-14.3
Intersection	Fe_3C-Fe_3B-$Fe_{1,2}Mn$	73.3–84.9	10.2–23.8	0.6–0.4	0.6–2.3
Eutectic	Fe-Mn-C	65.3-71.1	8.7-21.5	2.8-15.4	2.9-10.4
Intersection	"$Fe_{23}C_6$"-"$Fe_{23}B_6$"-"$Fe_{23}Mn_6$"	89.7–92.5 79.3	3.1–6.9 2.7-6.2	1.4–3.9 5.4-15.5	0.2–2.5 1.1-10.8

Quasi-ternary intersection		Content of elements*			
		Fe	Mn	C	B
Eutectic	Fe-Mn-C	89.7–92.5 79.3	3.1–6.9 2.7-6.2	1.4–2.9 5.4-10.9	0.7–2.5 3.6-10.8
Eutectic	Fe-B-C	89.7–92.5 79.3	3.1–6.7 2.7-6.1	2.8–3.9 10.7-15.5	0.2–1.5 1.1-6.8

*numerator: wt%, denominator: at%.

Table 7. Content of elements in eutectic areas of Fe_2C-Fe_2B-'Fe_2Mn', Fe_3C-Fe_3B-'Fe_3Mn', Fe_3C-Fe_3B-'$Fe_{1.2}Mn$', '$Fe_{23}C_6$'-'$Fe_{23}B_6$'-'$Fe_{23}Mn_6$' intersections of the Fe-Mn-B-C system.

Eutectic alloys are dispersion-reinforced composites with a structural gradient in which the soft matrix lamellar phase (alloying pearlite or austenite) is strengthened with hard and resistant $Fe_{0.4}Mn_{3.6}C$ phase. The structure and properties of the alloys can be controlled by changing the contents of their components. The alloying can be carried out with the majority of selected metallic elements in the periodic table over their wide concentrations. Carbon content in alloys, according to the Fe-Mn-C equilibrium diagram, can be changed in a broad range—0.6–6.4 wt%.

For the development of chemical composition of eutectic alloys, the examinations of the Fe-Mn-C-B phase equilibrium system were used to determine the eutectic areas (**Tables 3–6; Figures 1–5**). The composition of elements for the production of eutectic alloys of the Fe-Mn-C-B system is as follows (wt%):

Fe	86.6–97.4
Mn	2.2–13.0
C	0.4–1.5
B	2.9

The following content of elements in eutectic areas was identified by X-ray phase analysis after four quasi-ternary intersections (**Figure 1**; **Table 7**).

4. Conclusions

The following conclusions can be put forward based on the works performed:

(1) The analysis of the examined systems makes it possible to conclude that

(a) Fe-Mn-C eutectic exists at boron contents of 0.6–2.5 wt% and at the following contents of other elements:

Fe	73.3–92.5
Mn	1.6–23.8
C	0.6–7.0

http://dx.doi.org/10.5772/66873

(b) Fe-Mn-C-B eutectic forms at manganese contents of 1.6–7.6 wt% and at the following contents of other elements:

Fe	85.1–92.5
B	0.2–3.5
C	2.6–7.0

(2) There is a possibility of alloying the Fe-Mn-C-B system with virtually any elements in the periodic table over a wide range of their concentrations.

(3) By selection of chosen alloying elements, such as Si, Ni, Cr, it is possible to produce alloys with diverse physico-mechanical properties as a result of selection of various alloying components.

(4) Based on the examinations of the Fe-Mn-C-B system according to four quasi-ternary intersections and micro-X-ray examinations, the following content of elements in eutectic areas was identified (**Figure 1**; **Table 7**):

- Fe-B-C eutectic, at manganese content of 1.6–7.6%: 85.1–92.5 Fe; 0.2–3.5 B; 2.6–7.0 C;
- Fe-Mn-C eutectic, at boron content of 0.6–2.5%: 73.3–92.5 Fe; 3.1–23.8 Mn; 0.6–6.4 C.

In particular, the examinations of the Fe-Mn-C-B system after four quasi-ternary intersections: 'Fe_2C'-Fe_2B-'Fe_2Mn', Fe_3C-Fe_3B-'Fe_3Mn', Fe_3C-Fe_3B-'$Fe_{1.2}Mn$', '$Fe_{23}C$'-'$Fe_{23}B$'-'$Fe_{23}Mn$' and the X-ray analysis of the samples annealed at 1270 K for 350 h would make it possible to conclude as follows:

- Based on the X-ray and metallographic examinations, it has been determined that there are two phase areas at all quasi-ternary intersections, which correspond to ternary Fe-Mn-C and Fe-B-C systems (**Figure 1**): area I, Fe-B-C system: $Fe_3(C, B)$ + γ-(Fe, Mn) + α-(Fe, Mn); area II, Fe-Mn-C system: $(Fe, Mn)_{23}(C, B)_6$ + γ-(Fe, Mn) + α-(Fe, Mn).
- The alloys of the Fe_3C-Fe_3B-'$Fe_{1.2}Mn$' intersection at 0.667 at. parts of Fe contain no α-(Fe, Mn)-based phase. This phase was detected in alloys at intersections with increased iron content (0.75 atomic parts) only. It is the γ-(Fe, Mn) phase, which does not exist after quenching of samples from 1270 K.
- In eutectic alloys within the area of the highest iron content (0.79; 0.75 atomic parts), the $(Fe, Mn)_{23}(C, B)_6$ + α-(Fe, Mn) + γ-(Fe, Mn), $Fe_3(C, B)$ + α-(Fe, Mn) + γ-(Fe, Mn) phases are in equilibrium. With the reduction in iron content [0.667 atomic parts (Fe_3C-Fe_3B-'$Fe_{1.2}Mn$' intersection)], the transition from γ- into α-Fe does not occur and the $(Fe, Mn)_{23}(C, B)_6$ + γ-(Fe, Mn), $Fe_3(C, B)$ + γ-(Fe, Mn) phases are in equilibrium.
- The eutectic areas in 'Fe_2C'-Fe_2B-'Fe_2Mn', Fe_3C-Fe_3B'Fe_3Mn' and '$Fe_{23}C_6$-'$Fe_{23}B_6$'-'$Fe_{23}Mn_6$' quasi-ternary intersections were found in two phase areas, at the Fe_3C-Fe_3B-'$Fe_{1.2}Mn$' intersection—in area II (Fe-Mn-C eutectic). Generally, the Fe-B-C eutectic is formed in the area of increased carbon and boron contents, while the Fe-Mn-C eutectic is observed in the area of increased Mn content.

Author details

Mykhaylo Pashechko, Klaudiusz Lenik*, Joanna Szulżyk-Cieplak and Aneta Duda

*Address all correspondence to: wz.kpt@pollub.pl

Faculty of Fundamentals of Technology, Lublin University of Technology, Lublin, Poland

References

[1] Dobrzański L.A. Basics of Material Science Metal Science. Warsaw: WNT; 2002.

[2] Lenik K, Pashechko M. Development of a new family of wear-resistant eutectic alloys. In: Works of the Institute of Machine Design and Operation. No. 87. The 35th Tribology School, No. 27; Publishing House of the Wroclaw University of Technology; 2002. p. 196–201.

[3] Lenik K, editor. Anti-wear Eutectic Coatings of the Fe-Mn-C-B System. Lviv: The National Academy os Science of Ukraine, Institute on Problems of Materials Science, Euro World; 2004.

[4] Lenik K, Paszeczko M, Paszeczko L. Wear resistance eutectic composite coatings of system Fe-Mn-C-B-Si. Problems of Tribology. 2001;**3**:61–64.

[5] Jarzyna W, Augustyniak H, Bocheński H. Active Piezoelectric Structures in Control Systems. Przegląd Elektrochemiczny. 2010;**86(4):**252–255.

[6] Paszeczko M, Lenik K, Paszeczko L. Increased durability of machine parts by plasma deposition using eutectic alloys of Fe-Mn-C-B. In: II Mieżdunarodnaja N-T Konferencjja Nowyje technologii, metody obrabotki i uprocznienija dietalej energeticzeskich ustanowok; 23–28 sientiabria 2002; Zaporożje-Ałuszta, Zaporoski Państwowy Instytut 2002. p. 77–78.

[7] Paszeczko M, Lenik K, Szewczuk J. Pidwyszczennia znosostijkosti dyska kopacza korenezbyralnoji maszyny KS-6B nanesenniam ewtektycznych kompozycyjnych pokryttiw systemy Fe-Mn-C-B-Si-Cr. Problems of Tribology. 2003;**2**:154–157.

[8] Pashechko M, Gorecki T. Surface layer models and self-organisation of the surface with abrasive wear. In: Zagadnienia dydaktyczne w środowisku systemów technologicznych. Lublin: LTN. 2003. p. 157–162.

[9] Paszeczko M, Lenik K, Paszeczko L. Pidwyszczennia dowhowiczności detałej maszyn metodom płazmowogo napławlennia z wykorystanniam ewtektycznych spławiw systemy Fe-Mn-C-B. Westnik Dwigatelestrojenija. 2002;**1**:127–131.

[10] Paszeczko M, Popławskij O. Influence of surface atoms segregation on tribological properties of alloys. Problems of Tribology. 2001;**4**:115–125.

[11] Malec M, Lenik K, Pashechko M. The posibilities of increasing the lifetime of tools by using modified surface layer. In: The 7th National Conference on Tool Problems in Plastic Working. Bydgoszcz. 2001. p. 87–93.